Hybrid High-Temperature-Superconductor–Semiconductor Tunnel Diode

Alex Hayat,[1,2] Parisa Zareapour,[1] Shu Yang F. Zhao,[1] Achint Jain,[1] Igor G. Savelyev,[3] Marina Blumin,[3] Zhijun Xu,[4] Alina Yang,[4] G. D. Gu,[4] Harry E. Ruda,[2,3] Shuang Jia,[5] R. J. Cava,[5] Aephraim M. Steinberg,[1,2] and Kenneth S. Burch[1]

[1]*Department of Physics and Institute for Optical Sciences, University of Toronto, Toronto, Ontario M5S 1A7, Canada*

[2]*Centre for Quantum Information and Quantum Control, University of Toronto, 60 St. George Street, Toronto, Ontario M5S 1A7, Canada*

[3]*Centre for Advanced Nanotechnology and Institute for Optical Sciences, University of Toronto, 170 College Street, Toronto, Ontario M53 3E4, Canada*

[4]*Condensed Matter Physics and Materials Science Department, Brookhaven National Laboratory, Upton, New York 11973, USA*

[5]*Department of Chemistry, Princeton University, Princeton, New Jersey 08544, USA*

(Received 14 April 2012; revised manuscript received 19 October 2012; published 27 December 2012)

We report the demonstration of hybrid high-T_c-superconductor–semiconductor tunnel junctions, enabling new interdisciplinary directions in condensed matter research. The devices are fabricated by our newly developed mechanical-bonding technique, resulting in high-T_c-superconductor–semiconductor tunnel diodes. Tunneling-spectra characterization of the hybrid junctions of $Bi_2Sr_2CaCu_2O_{8+\delta}$ combined with bulk GaAs, or a GaAs/AlGaAs quantum well, exhibits excess voltage and nonlinearity, similarly to spectra obtained in scanning-tunneling microscopy, and is in good agreement with theoretical predictions for a *d*-wave-superconductor–normal-material junction. Additional junctions are demonstrated using $Bi_2Sr_2CaCu_2O_{8+\delta}$ combined with graphite or Bi_2Te_3. Our results pave the way for new methods in unconventional superconductivity studies, novel materials, and quantum technology applications.

DOI: 10.1103/PhysRevX.2.041019 Subject Areas: Electronics, Semiconductor Physics, Superconductivity

Superconductors enable the implementation of fast ultrasensitive detectors [1,2] and large-scale quantum-computation technology [3,4]. These materials pose major scientific and technological challenges, however. A potential alternative avenue may be provided by hybrid semiconductor-superconductor devices, which have been attracting growing attention lately as they combine the controllability of semiconductor structures with the macroscopic quantum states of superconductors [5,6]. The interaction of light with semiconductor-superconductor structures has recently emerged as a new interdisciplinary field of superconducting optoelectronics, with demonstrations of light emission from hybrid light-emitting diodes [7,8] enhanced by the superconducting state [9,10], and various proposals for novel lasers [11] and quantum light sources [12,13]. These hybrid devices have also proven useful in nonlinear electronics [14,15] and infrared detection [16], taking advantage of the relatively small size of the superconducting gap in the tunneling spectrum [17]. All previously studied semiconductor-superconductor devices were based on conventional low-critical-temperature (low-T_c) superconductors, requiring cooling to extremely low temperatures. Moreover, the small superconducting gaps of these materials limit the energy scales over which they can be employed. A high operating temperature and large *d*-wave gaps can be obtained by incorporating unconventional high-T_c superconductors [18,19] that exhibit a variety of novel phenomena and provide a more practical alternative for device implementation. Furthermore, by combining high-T_c materials with semiconductors, one could take advantage of mature semiconductor technology to probe the unconventional nature of high-T_c superconductors [20] in hybrid tunneling junctions.

Tunneling spectroscopy is among the most widely used techniques for the study of novel materials and new phenomena in condensed matter physics [21]. Various effects have been observed with tunneling spectroscopy such as weak localization [22], superconducting-gap dependence on a magnetic field [23], bound states and broken symmetries in high-T_c superconductors [24], as well as studies of the pseudogap, preformation of Cooper pairs [25], and electron-hole asymmetry [26]. These experiments usually require sophisticated and expensive scanning-tunneling spectroscopy equipment. A simple method of constructing high-T_c tunnel junctions may create a new conceptual paradigm for tunneling-spectroscopy studies of these unconventional materials. Hybrid semiconductor-high-T_c optoelectronic devices such as superconducting light sources [12,13] could help shed new light on the physics of high-T_c materials by demonstrating photon-pair emission from Cooper pairs above T_c, which is still a hotly debated issue [27]. The realization of such devices has been prevented, however, by the fact that high-T_c epitaxial

layers can be grown only on a very limited range of substrates.

Here we demonstrate a hybrid high-T_c-superconductor–semiconductor device, namely, a superconducting tunnel diode constructed from $Bi_2Sr_2CaCu_2O_{8+\delta}$ (Bi-2212) combined with bulk GaAs, a GaAs/AlGaAs quantum well (QW), graphite, or Bi_2Te_3. The devices are fabricated by our newly developed method of mechanically bonded planar junctions, and characterized by DC current voltage [current (I) measured vs voltage (V), here indicated by I-V] and AC differential-conductance measurements. Similar to work previously developed and studied on low-T_c hybrid structures, these junctions reveal nonlinear current-voltage characteristics and excess voltage [28]. These are unique features resulting from the gap in the superconductor quasiparticle-excitation spectrum. These features as well as a broadening of the tunneling spectrum by quasiparticle scattering are in good agreement with the *d*-wave superconductor–normal-material-junction theory [29]. We also show similar nonlinearity and excess voltage in graphite-based junctions and junctions based on Bi_2Te_3—a novel material that has recently been shown to have topologically protected surface states [30]. The fact that the agreement between theory and experiment holds in a wide array of normal materials (GaAs, graphite, Bi_2Te_3) with very different normal-state properties demonstrates the robustness of this technique for studying high-T_c superconductors.

The hybrid planar junctions are constructed by our newly developed mechanical-bonding technique, enabling the implementation of semiconductor-high-T_c devices. This method provides a unique and simple solution for combinations of novel materials that cannot be achieved by conventional approaches. The simplicity of the fabrication method, which does not require expensive facilities, and the resulting devices, which can operate at temperatures of liquid nitrogen, make this approach technologically practical and also greatly expand the range of possible experiments in the field of high-T_c superconductivity. The device fabrication is achieved using Bi-2212 crystals grown by the floating-zone method [31]. The Bi-2212 is cleaved in a nitrogen-purged dry box with adhesive tape producing atomically flat surfaces over large areas. Subsequently, it is mechanically bonded to a *p*-doped (where the carrier density is greater than 5×10^{18} cm^{-3}) bulk GaAs or a GaAs/AlGaAs QW, where the doping is required to reduce the effect of the Schottky barrier. The mechanical bonding is achieved by freshly cleaving Bi-2212 in a dry atmosphere, and then rapidly pressing it onto the semiconductor surface. The Bi-2212 crystals used in the measurements presented here are rectangular samples about 1 mm^2 in area and several hundreds of μm in thickness. To confirm that surface forces are strong enough to guarantee good contact between the two materials, we have first mechanically exfoliated nanocrystals of Bi-2212 [32] on top of GaAs. However, due to the difficulty of performing

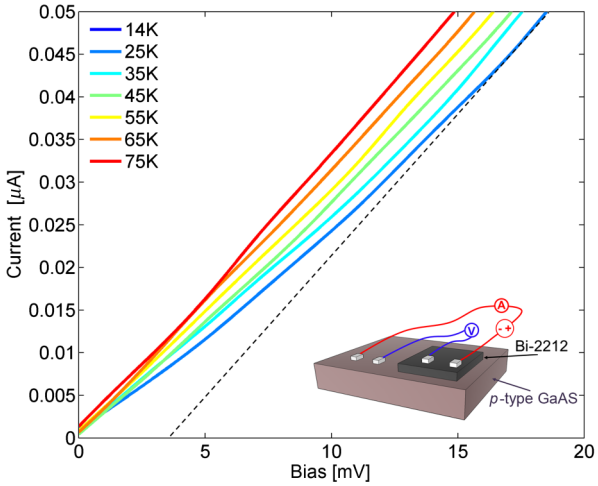

FIG. 1. Measured DC I-V characteristics for the Bi-2212/GaAs junction at various temperatures. The dashed line indicates a linear I-V dependence coinciding with the 14-K measurement at a higher bias to indicate the excess voltage. The inset is a schematic drawing of the Bi-2212/GaAs device.

conductance measurements on exfoliated nanocrystals, we have chosen to focus our initial efforts on bulk crystals (Fig. 1, inset). The larger samples should also have increased surface forces holding the GaAs and Bi-2212 together. Nonetheless, due to the increased volume-to-surface-area ratio of the bulk crystal, we have found that it is necessary to apply General Electric varnish to the edges of the Bi-2212 to secure the bonding. The exact Bi-2212/GaAs contact area is difficult to determine, because the atomically flat regions are smaller than the area of the entire crystal. However, judging from our successful mechanical exfoliation of Bi-2212 on GaAs, as well as the atomic force microscopy of the crystal surface, a large fraction of the Bi-2212 sample surface is in contact with the GaAs substrate.

To probe the interface with four-point differential-conductance measurements, contacts are made on the top of the bulk Bi-2212 and the semiconductor substrate using Cu wires and Ag epoxy. To confirm that we are only probing tunneling at the interface, different in-plane geometries of the contacts are tested without any effect of the geometry on the measurements. All the processing steps besides crystal growth are performed at room temperature, and the key requirement is to perform them in a clean and dry atmosphere—in our case, in a nitrogen-purged glove box. The differential-conductance-spectroscopy measurements include both DC current-voltage characteristics and AC differential conductance versus voltage. The temperature-dependent measurements are performed using a liquid He flow cryostat.

The first set of measurements is performed on Bi-2212/bulk-GaAs junctions. The Bi-2212 crystals on GaAs are measured to be slightly underdoped ($T_c \sim 70$ K). The reduced doping of Bi-2212 crystals can result partially

from the diffusion of oxygen interstitials due to the oxidation of the GaAs surface. Differential AC conductance and DC I-V characteristics at different temperatures are measured on the junction using two lock-in amplifiers (Stanford Research Systems SR810) and a DC voltage source (BK Precision 1787B). The measurements are current polarized where the current source is implemented using a DC voltage source with a large resistor. The AC voltage from one of the lock-in amplifiers is added to the DC output of the power supply using a shielded transformer-based adder. The AC + DC voltage is applied to the sample, and the resulting voltage drop is measured with a lock-in amplifier (the AC part) and a multimeter (the DC part). The current is converted to voltage and measured with another lock-in amplifier (AC) and a multimeter (DC) using a preamplifier (SRS 570). The small amplifier offset results in a slightly nonzero current at zero bias in DC measurements, which is much smaller than the important measured values such as the current corresponding to the excess voltage.

Studying the temperature dependence of the I-V characteristics of the Bi-2212/GaAs bulk junction (Fig. 1) shows that, for temperatures above T_c, the junction behaves almost as a normal Ohmic resistor R_n. Above T_c, the I-V can be slightly nonlinear due the effect of the pseudogap, which is common amongst high-T_c superconductors [33]. As the junction is cooled below T_c, the I-V characteristics become significantly nonlinear due to the reduction of the tunneling probability for single quasiparticle excitations when the superconducting gap opens up in the density of states of Bi-2212. The nonlinear low-temperature I-V dependence becomes linear for higher bias voltages; however, it is displaced from the normal I-V characteristic by the excess voltage $V_e = V - R_n I$ [28]. This displacement from normal linear I-V dependence can be extracted by extrapolating the linear part of the low-temperature curve in a positive bias to the axis (Fig. 1 dashed line). The extracted excess voltage decreases with increasing temperature due to the reduction of the Bi-2212 gap.

A direct measurement of the superconducting gap is also performed by AC differential conductance. Below T_c, the ratio of the differential conductance $[dI/dV]_S$, to the normal-state conductance $[dI/dV]_N$ demonstrates the temperature dependence of the superconducting gap of Bi-2212 (Fig. 2), and resembles point-contact and scanning-tunneling measurements taken on bulk Bi-2212 [34,35]. The data is consistent with that expected for an underdoped sample [36]. The pair potential in Bi-2122 is d wave and thus highly anisotropic in the ab plane [37]. Thus, in our c-axis tunneling experiment, an averaged V-shaped gap appears with the maximal value close to 20 mV. Again, the appearance of the gap is consistent with our inference that Bi-2212 is underdoped. The excess voltage should be proportional to, yet smaller than, the maximal value observed in the V-shaped gap even at low temperatures (see Figs. 1 and 2).

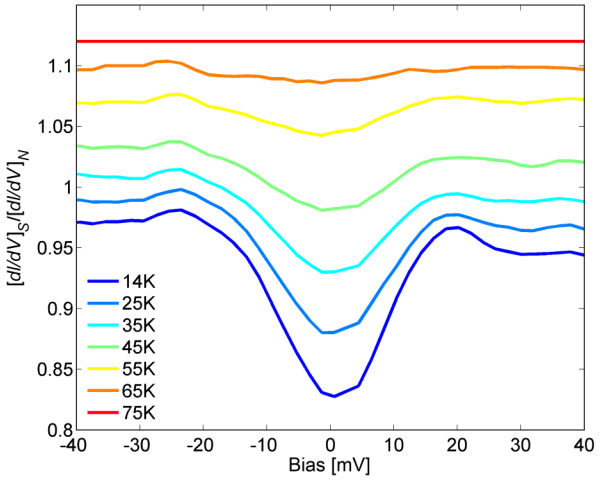

FIG. 2. Measured AC differential conductance below T_c $[dI/dV]_S$, divided by the normal-state conductance $[dI/dV]_N$ for the Bi-2212/GaAs junction at various temperatures. The curves are shifted vertically for clarity by 2%, and the vertical axis corresponds to the 14-K curve.

At low temperatures the depth of the gap, the sharpness of the features in the differential conductance, and the nonlinearity of the I-V characteristics are determined by the scattering rates of the quasiparticles in the normal material [38]. Carrier scattering rates in bulk GaAs are typically faster than 1 ps^{-1} [39] leading to an energy broadening of more than 10 meV. This broadening significantly reduces the excess voltage in the I-V characteristics and the depth of the gap-induced dip in the differential-conductance measurements.

Two-dimensional structures such as InAs/AlSb QWs have been shown to exhibit highly nonlinear I-V characteristics with low-T_c Nb-based structures [40]. It has been shown recently that Dynes broadening is affected by electromagnetic dissipation [41]. We show here that a different type of dissipation, namely, inelastic scattering of quasiparticles, has a significant effect on the tunneling spectrum. Specifically, the scattering rate is determined by the dimensionality of the semiconductor structure. QWs can have much longer carrier scattering times than those of bulk materials [42], even in the presence of intersubband transitions [43], resulting in smaller broadening, stronger I-V nonlinearities, and larger excess voltages. In addition, by introducing a QW into the structure, one gains a significant degree of freedom in tuning the overall properties of the junction, which can be crucial for device design.

In order to enhance the superconducting tunnel effect, we designed and fabricated Bi-2212/GaAs/AlGaAs junctions with a GaAs QW. The Be-doped GaAs QW (10-nm thick) is grown by molecular beam epitaxy on a Si-doped $Al_{0.25}Ga_{0.75}As$ barrier (100-nm thick), which itself has been grown by molecular beam epitaxy on an n^+ GaAs substrate. The counterdoped barrier results in band bending, which provides an additional confinement of the holes

to the interface region [Fig. 3(b)] and results in a reduction in inelastic tunneling. The superconductor-normal-material junction is in the direction of growth in the semiconductor, and along the c axis of Bi-2212. However, below the superconductor-normal vertical junction, the transport inside GaAs is between the contacts separated in the lateral direction on top of the GaAs sample [Fig. 1, inset; Fig. 3(a)]. In the QW-based junction with the additional carrier confinement obtained with the counterdoping-based band bending, the transport is even more well defined to be in-plane [Fig. 3(b)]. Below T_c, the measured I-V characteristics for a Bi-2212/GaAs/AlGaAs QW junction exhibit the nonlinear I-V dependence and excess voltage induced by quasiparticle tunneling [Fig. 3(c)]. Above T_c, the I-V dependence is linear, as expected from a superconducting tunnel diode. However, the nonlinearity below T_c in a QW-based junction is much stronger than in the bulk-GaAs junction (Fig. 1), and the excess voltages V_e are larger than 10 mV. The enhanced excess voltages in QW junctions are caused by the reduced scattering rate in the two-dimensional QW system, which results in a stronger effect of the superconducting gap of Bi-2212 on the tunneling spectra.

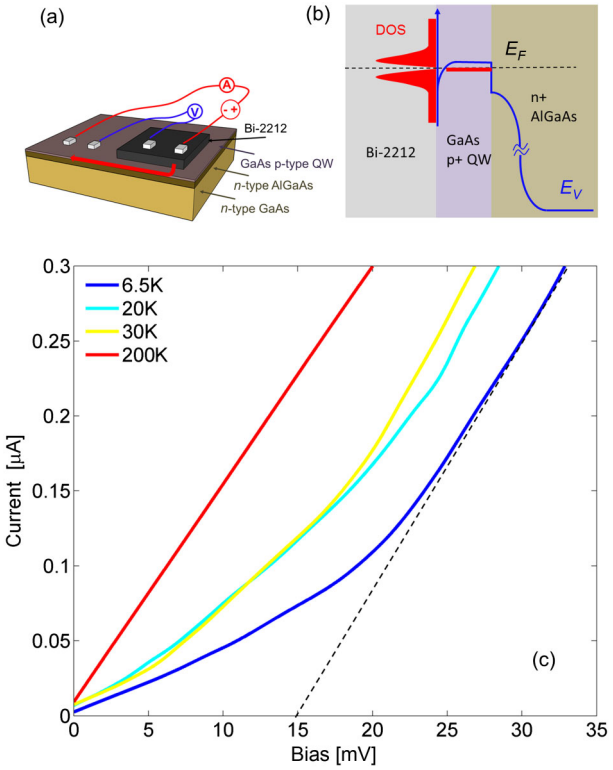

FIG. 3. (a) Schematic drawing of the Bi-2212/GaAs/AlGaAs device. (b) Energy diagram of the device. (c) Measured DC I-V characteristics for the Bi-2212/GaAs/AlGaAs junction at various temperatures. The dashed line indicates a linear I-V dependence coinciding with the 6.5-K measurement at a higher bias to indicate the excess voltage.

To model the effect quantitatively, we calculate the c-axis Bi-2212/GaAs and Bi-2212/GaAs/AlGaAs QW tunneling spectra using an extension of the Blonder-Tinkham-Klapwijk superconductor–normal-interface formalism [44], developed for anisotropic superconductors [29]. The ratio of the differential conductance $[dI/dV]_S$ to the normal-state conductance $[dI/dV]_N$ is given by the half-sphere integration over solid angle Ω,

$$\sigma(E) = \frac{\int d\Omega \sigma_N \cos\theta_N \sigma_R(E)}{\int d\Omega \sigma_N \cos\theta_N}, \tag{1}$$

where E and θ_N are the quasiparticle energy and incidence angle in the normal material, respectively, σ_N is the conductance from normal-to-normal material with the same geometry, and

$$\sigma_R(E) = \frac{1 + \sigma_N|\kappa_+|^2 + (\sigma_N - 1)|\kappa_-\kappa_+|^2}{|1 + (\sigma_N - 1)|\kappa_-\kappa_+|\exp(i\varphi_- - i\varphi_+)|^2}, \tag{2}$$

with

$$\kappa_\pm = [E + i\Gamma - \sqrt{(E + i\Gamma)^2 - |\Delta_\pm|^2}]/|\Delta_\pm|, \tag{3}$$

and $\Delta_\pm = |\Delta_\pm|\exp(i\varphi_\pm)$ are electronlike and holelike quasiparticle effective pair potentials with the corresponding phases $i\varphi_\pm$. The calculations are performed with equal maximal values of the gap and the barrier for both the bulk and the QW-based junctions, while the scattering-induced energy broadening $i\Gamma$ is included in the calculation as a fitting parameter. The origin of this broadening term in tunneling experiments is not always clear. However, recent studies have shown that, when a superconductor is coupled to a dissipative environment, the Dynes broadening can be explained mostly by quasiparticles exchanging energy with the environment during tunneling, and a recent experiment has demonstrated the effect of electromagnetic radiation on the Dynes broadening [41].

In our case, the QW and the bulk GaAs are the primary sources of inelastic scattering in the tunneling, acting therefore as the environment. The quasiparticles can exchange energy with phonons or charge carriers in the semiconductor during tunneling. Scattering in the semiconductor, therefore, can contribute a significant portion of the broadening, Γ. Other dissipative processes during tunneling could also contribute to the broadening; however, the main difference between the QW and the bulk-GaAs experiments is the effect of the dimensionality of the semiconductor on the dissipative-scattering rates.

Our calculations according to this model are consistent (within a few percent) with the experimental results (Fig. 4). The difference between the density of states in the two different kinds of normal materials, namely, bulk GaAs and the QW, is accounted for by normalizing each to the normal conductance above T_c. The large quasiparticle energy broadening in bulk GaAs significantly reduces the depth of the superconducting gap, resulting in a smaller

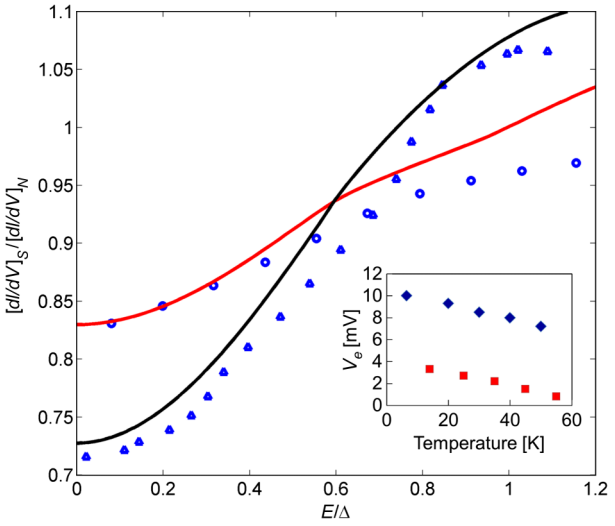

FIG. 4. AC differential conductance $[dI/dV]_S$ at 14 K, divided by the normal-state conductance $[dI/dV]_N$ for the Bi-2212/GaAs junction measured (circles) and calculated (solid red) with the $\Gamma = 15$ meV, and for the Bi-2212/GaAs/AlGaAs junction measured (triangles) and calculated (solid black) with the $\Gamma = 6$ meV. The inset is the excess voltage vs temperature in a bulk-GaAs device (red squares) and in the QW-based device (blue diamonds).

excess voltage (Fig. 1). In contrast, the reduced scattering rate in the two-dimensional GaAs/AlGaAs quantum well system enhances both the dip in the differential conductance (Fig. 4) and the excess voltage [Fig. 3(c)]. The larger nonlinearity in the QW-based device relative to the bulk device persists at much higher temperatures resulting in larger excess voltages (Fig. 4, inset).

To demonstrate the broad applicability of our technology, we have constructed superconducting tunnel junctions from additional materials. The third type of material we have used to construct a superconducting-normal junction is bulk graphite. A mechanically bonded junction of Bi-2212 on graphite exhibits excess voltage [Fig. 5(a)] similar to that obtained in GaAs-based junctions. The Bi-2212 in this junction is also slightly underdoped, resulting in a correspondingly smaller gap [Fig. 5(a), inset] and slightly lower T_c. The fourth material we have employed for the normal side of the high-T_c diode is Bi_2Te_3. In this experiment, an optimally doped Bi-2212 is mechanically bonded with Bi_2Te_3 [45]. The larger gap of an optimally doped Bi-2212 [Fig. 5(b), inset] results in enhanced nonlinearity and excess voltage as large as 25 mV [Fig. 5(b)].

The mechanical-bonding method presented here is reproduced in several different heterostructures. These results suggest wide applicability of the method; however, they do not yet constitute proof of universality. Extensions of our approach to other material classes have to be carefully studied, and will have to address the need to achieve controllable and reproducible interfaces in each specific case while employing the bonding technique.

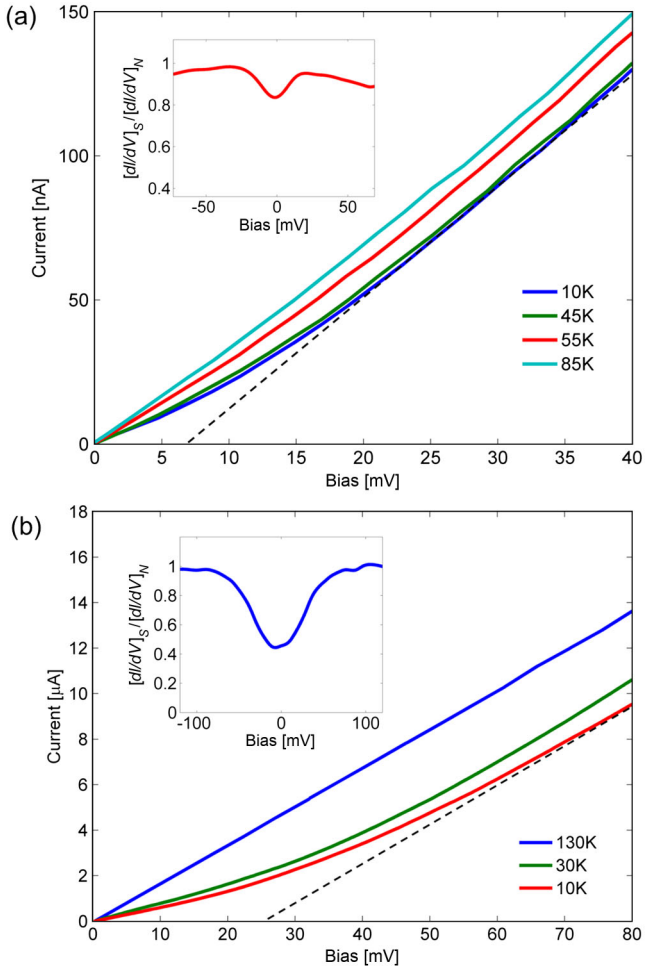

FIG. 5. (a) Measured DC I-V characteristics for the Bi-2212/graphite junction at various temperatures. The dashed line indicates a linear I-V dependence coinciding with the 10-K measurement at a higher bias to indicate the excess voltage. The inset is the measured differential conductance $[dI/dV]_S$ at 10 K, divided by the normal-state conductance $[dI/dV]_N$ for the Bi-2212/graphite junction. (b) Measured DC I-V characteristics for the Bi-2212/Bi_2Te_3 junction at various temperatures. The dashed line indicates a linear I-V dependence coinciding with the 10-K measurement at higher bias to indicate the excess voltage. The inset is the measured differential conductance $[dI/dV]_S$ at 10 K, divided by the normal-state conductance $[dI/dV]_N$ for the Bi-2212/Bi_2Te_3 junction.

In conclusion, we have demonstrated hybrid high-T_c-superconductor–semiconductor devices, which are fabricated by our newly developed method of mechanically bonded planar junctions. This technique is substantially different from previous work on low-T_c-semiconductor-superconductor hybrid devices, providing a unique solution for combinations of various novel materials unobtainable by conventional means. This method allows simple room-temperature fabrication of devices based on various easily cleavable crystals, including combinations of high-T_c superconductors such as Bi-2212 with graphite, Bi_2Se_3, and Bi_2Te_3.

The devices we have demonstrated here are junctions constructed from Bi-2212 combined with bulk GaAs, GaAs/AlGaAs quantum wells, graphite, or Bi_2Te_3 acting as superconducting tunnel diodes. The tunneling-spectra characterization of the hybrid junctions exhibits excess voltage and nonlinearity in DC I-V measurements as well as a decrease in conductance due to the Bi-2212 superconducting gap in AC differential-conductance measurements, in good agreement with theory. Additional junctions that are constructed from Bi-2212 combined with graphite or Bi_2Te_3 also show excess voltage and nonlinearity. These results enable practical high-T_c-hybrid-superconductor–semiconductor devices with new insights into fundamental studies of novel materials as well as applications in optoelectronics and quantum technologies.

The work at the University of Toronto was supported by the Natural Sciences and Engineering Research Council of Canada, the Canadian Foundation for Innovation, and the Ontario Ministry for Innovation. The crystal growth at Princeton was supported by the U.S. National Science Foundation, Grant No. DMR-0819860.

[1] A. J. Miller, S. W. Nam, J. M. Martinis, and A. V. Sergienko, *Demonstration of a Low-Noise Near-Infrared Photon Counter with Multiphoton Discrimination*, Appl. Phys. Lett. **83**, 791 (2003).

[2] H. Takesue, S. W. Nam, Q. Zhang, R. H. Hadfield, T. Honjo, K. Tamaki, and Y. Yamamoto, *Quantum Key Distribution over a 40-dB Channel Loss Using Superconducting Single-Photon Detectors*, Nat. Photonics **1**, 343 (2007).

[3] A. Blais, Ren-Shou Huang, Andreas Wallraff, S. M. Girvin, and R. J. Schoelkopf, *Cavity Quantum Electrodynamics for Superconducting Electrical Circuits: An Architecture for Quantum Computation*, Phys. Rev. A **69**, 062320 (2004).

[4] J. Clarke and F. K. Wilhelm, *Superconducting Quantum Bits*, Nature (London) **453**, 1031 (2008).

[5] S. De Franceschi, L. Kouwenhoven, C. Schönenberger, and W. Wernsdorfer, *Hybrid Superconductor–Quantum Dot Devices*, Nat. Nanotechnol. **5**, 703 (2010).

[6] G. Katsaros, P. Spathis, M. Stoffel, F. Fournel, M. Mongillo, V. Bouchiat, F. Lefloch, A. Rastelli, O. G. Schmidt, and S. De Franceschi, *Hybrid Superconductor-Semiconductor Devices Made from Self-Assembled SiGe Nanocrystals on Silicon*, Nat. Nanotechnol. **5**, 458 (2010).

[7] H. Sasakura, S. Kuramitsu, Y. Hayashi, K. Tanaka, T. Akazaki, E. Hanamura, R. Inoue, H. Takayanagi, Y. Asano, C. Hermannstädter, H. Kumano, and I. Suemune, *Enhanced Photon Generation in a* Nb/n-InGaAs/p-InP *Superconductor/Semiconductor-Diode Light Emitting Device*, Phys. Rev. Lett. **107**, 157403 (2011).

[8] I. Suemune, Y. Hayashi, S. Kuramitsu, K. Tanaka, T. Akazaki, H. Sasakura, R. Inoue, H. Takayanagi, Y. Asano, E. Hanamura, S. Odashima, and H. Kumano, *A Cooper-Pair Light-Emitting Diode: Temperature Dependence of Both Quantum Efficiency and Radiative Recombination Lifetime*, Appl. Phys. Express **3**, 054001 (2010).

[9] Y. Asano, I. Suemune, H. Takayanagi, and E. Hanamura, *Luminescence of a Cooper Pair*, Phys. Rev. Lett. **103**, 187001 (2009).

[10] P. Recher, Y. V. Nazarov, and L. P. Kouwenhoven, *Josephson Light-Emitting Diode*, Phys. Rev. Lett. **104**, 156802 (2010).

[11] F. Godschalk, F. Hassler, and Y. V. Nazarov, *Proposal for an Optical Laser Producing Light at Half the Josephson Frequency*, Phys. Rev. Lett. **107**, 073901 (2011).

[12] I. Suemune, T Akazaki, K. Tanaka, M. Jo, K. Uesugi, M. Endo, H. Kumano, E. Hanamura, H. Takayanagi, M. Yamanishi, and H. Kan, *Superconductor-Based Quantum-Dot Light-Emitting Diodes: Role of Cooper Pairs in Generating Entangled Photon Pairs*, Jpn. J. Appl. Phys. **45**, 9264 (2006).

[13] M. Khoshnegar and A. H. Majedi, *Entangled Photon Pair Generation in Hybrid Superconductor-Semiconductor Quantum Dot Devices*, Phys. Rev. B **84**, 104504 (2011).

[14] M. McColl, R. J. Pedersen, M. F. Bottjer, M. F. Millea, A. H. Silver, and F. L. Vernon, *The Super-Schottky Diode Microwave Mixer*, Appl. Phys. Lett. **28**, 159 (1976).

[15] M. Mück, Th. Becker, and C. Heiden, *Use of Super Schottky Diodes in a Cryogenic Radio Frequency Superconducting Quantum Interference Device Readout*, Appl. Phys. Lett. **66**, 376 (1995).

[16] M. McColl, M. F. Millea, and A. H. Silver, *The Superconductor-Semiconductor Schottky Barrier Diode Detector*, Appl. Phys. Lett. **23**, 263 (1973).

[17] A. Kastalsky, A. W. Kleinsasser, L. H. Greene, R. Bhat, F. P. Milliken, and J. P. Harbison, *Observation of Pair Currents in Superconductor-Semiconductor Contacts*, Phys. Rev. Lett. **67**, 3026 (1991).

[18] D. N. Basov and T. Timusk, *Electrodynamics of High-T_c Superconductors*, Rev. Mod. Phys. **77**, 721 (2005).

[19] P. A. Lee, N. Nagaosa, and X.-G. Wen, *Doping a Mott Insulator: Physics of High Temperature Superconductivity*, Rev. Mod. Phys. **78**, 17 (2006).

[20] T. Van Duzer, *Superconductor–Semiconductor Hybrid Devices, Circuits and Systems*, Cryogenics **28**, 527 (1988).

[21] D. A. Bonnell, *Scanning Probe Microscopy and Spectroscopy: Theory, Techniques, and Applications* (Wiley-VCH, New York, 2001), 2nd ed.

[22] W. Poirier, M. Sanquer, and K. Saminadayar, *Weak Localization and Interaction in Doped CdTe*, Eur. Phys. J. B **8**, 293 (1999).

[23] S. I. Vedeneev, B. A. Piot, and D. K. Maude, *Magnetic Field Dependence of the Superconducting Energy Gap in* $Bi_2Sr_2CaCu_2O_{8+\delta}$ *Probed Using Break-Junction Tunneling Spectroscopy*, Phys. Rev. B **81**, 054501 (2010).

[24] L. H. Greene, P. Hentges, H. Aubin, M. Aprili, E. Badica, M. Covington, M. M. Pafford, G. Westwood, W. G. Klemperer, S. Jian, and D.G. Hinks, *Planar Tunneling Spectroscopy of High-Temperature Superconductors: Andreev Bound States and Broken Symmetries*, Physica (Amsterdam) **387C**, 162 (2003).

[25] O. Yuli, I. Asulin, Y. Kalcheim, G. Koren, and O. Millo, *Proximity-Induced Pseudogap: Evidence for Preformed Pairs*, Phys. Rev. Lett. **103**, 197003 (2009).

[26] J. Nieminen, H. Lin, R. S. Markiewicz, and A. Bansil, *Origin of the Electron-Hole Asymmetry in the Scanning Tunneling Spectrum of the High-Temperature* $Bi_2Sr_2CaCu_2O_{8+\delta}$ *Superconductor*, Phys. Rev. Lett. **102**, 037001 (2009).

[27] O. Cyr-Choinière, R. Daou, F. Laliberté, D. LeBoeuf, N. Doiron-Leyraud, J. Chang, J.-Q. Yan, J.-G. Cheng, J.-S. Zhou, J. B. Goodenough, S. Pyon, T. Takayama, H. Takagi, Y. Tanaka, and L. Taillefer, *Enhancement of the Nernst Effect by Stripe Order in a High-*T_c *Superconductor*, Nature (London) **458**, 743 (2009); L. Li, Y. Wang, S. Komiya, S. Ono, Y. Ando, G. D. Gu, and N. P. Ong, *Diamagnetism and Cooper Pairing above* T_c *in Cuprates*, Phys. Rev. B **81**, 054510 (2010).

[28] A. W. Kleinsasser and A. Kastalsky, *Excess Voltage and Resistance in Superconductor-Semiconductor Junctions*, Phys. Rev. B **47**, 8361 (1993).

[29] S. Kashiwaya, Y. Tanaka, M. Koyanagi, and K. Kajimura, *Theory for Tunneling Spectroscopy of Anisotropic Superconductors*, Phys. Rev. B **53**, 2667 (1996).

[30] Y. L. Chen, J. G. Analytis, J.-H. Chu, Z. K. Liu, S.-K. Mo, X. L. Qi, H. J. Zhang, D. H. Lu, X. Dai, Z. Fang, S. C. Zhang, I. R. Fisher, Z. Hussain, and Z.-X. Shen, *Experimental Realization of a Three-Dimensional Topological Insulator,* Bi_2Te_3, Science **325**, 178 (2009).

[31] G. D. Gu, K. Takamuku, N. Koshizuka, S. Tanaka, *Growth and Superconductivity of* $Bi_{2.1}Sr_{1.9}Ca_{1.0}(Cu_{1-y}Fe_y)_2O_x$ *Single Crystal*, J. Cryst. Growth **137**, 472 (1994).

[32] L. J. Sandilands, J. X. Shen, G. M. Chugunov, S. Y. F. Zhao, S. Ono, K. S. Burch, *Stability of Exfoliated* $Bi_2Sr_2Dy_xCa_{1-x}Cu_2O_{8+\delta}$ *Studied by Raman Microscopy*, Phys. Rev. B **82**, 064503 (2010).

[33] T. Timusk and B. Statt, *The Pseudogap in High-Temperature Superconductors: An Experimental Survey*, Rep. Prog. Phys. **62**, 61 (1999).

[34] G. Deutscher, *Andreev–Saint-James Reflections: A Probe of Cuprate Superconductors*, Rev. Mod. Phys. **77**, 109 (2005).

[35] A. N. Pasupathy, A. Pushp, K. K. Gomes, C. V. Parker, J. Wen, Z. Xu, G. Gu, S. Ono, Y. Ando, and A. Yazdani, *Electronic Origin of the Inhomogeneous Pairing Interaction in the High-*T_c *Superconductor* $Bi_2Sr_2CaCu_2O_{8+\delta}$, Science **320**, 196 (2008).

[36] Y. Kohsaka, C. Taylor, P. Wahl, A. Schmidt, J. Lee, K. Fujita, J. W. Alldredge, K. McElroy, Jinho Lee, H. Eisaki, S. Uchida, D. -H. Lee, and J. C Davis, *How Cooper Pairs Vanish Approaching the Mott Insulator in* $Bi_2Sr_2CaCu_2O_{8+\delta}$, Nature (London) **454**, 1072 (2008).

[37] I. M. Vishik, W. S. Lee, R-H. He, M. Hashimoto, Z. Hussain, T. P. Devereaux and Z-X. Shen, *ARPES Studies of Cuprate Fermiology: Superconductivity, Pseudogap and Quasiparticle Dynamics*, New J. Phys. **12**, 105008 (2010).

[38] R. C. Dynes, V. Narayanamurti, and J. P. Garno, *Direct Measurement of Quasiparticle-Lifetime Broadening in a Strong-Coupled Superconductor*, Phys. Rev. Lett. **41**, 1509 (1978).

[39] D. W. Snoke, *Density Dependence of Electron Scattering at Low Density*, Phys. Rev. B **50**, 11583 (1994).

[40] C. Nguyen, H. Kroemer, and E. L. Hu, *Anomalous Andreev Conductance in InAs-AlSb Quantum Well Structures with Nb Electrodes*, Phys. Rev. Lett. **69**, 2847 (1992).

[41] J. P. Pekola, V. F. Maisi, S. Kafanov, N. Chekurov, A. Kemppinen, Yu. A. Pashkin, O.-P. Saira, M. Möttönen, and J. S. Tsai, *Environment-Assisted Tunneling as an Origin of the Dynes Density of States*, Phys. Rev. Lett. **105**, 026803 (2010).

[42] J. A. Kash, *Carrier-Carrier Scattering: An Experimental Comparison of Bulk GaAs and* $GaAs/Al_xGa_{1-x}As$ *Quantum Wells*, Phys. Rev. B **48**, 18336 (1993).

[43] M. Hartig, S. Haacke, P. E. Selbmann, B. Deveaud, R. A. Taylor, and L. Rota, *Efficient Intersubband Scattering via Carrier-Carrier Interaction in Quantum Wells*, Phys. Rev. Lett. **80**, 1940 (1998).

[44] G. E. Blonder, M. Tinkham, and T. M. Klapwijk, *Transition from Metallic to Tunneling Regimes in Superconducting Microconstrictions: Excess Current, Charge Imbalance, and Supercurrent Conversion*, Phys. Rev. B **25**, 4515 (1982).

[45] P. Zareapour, A. Hayat, S. Y. F. Zhao, M. Kreshchuk, A. Jain, D. C. Kwok, N. Lee, S.-W. Cheong, Z. Xu, A. Yang, G. D. Gu, R. J. Cava, and K. S. Burch, *Proximity-Induced High-Temperature Superconductivity in Topological Insulators Bi2Se3 and Bi2Te3*, Nat. Commun. **3**, 1056 (2012).